

MINISTÉRIO DA CIÊNCIA E TECNOLOGIA
INSTITUTO NACIONAL DE PESQUISAS ESPACIAIS

INPE-8070-PRE/3886

**MONTE-CARLO ANALYSIS OF NONIMPULSIVE ORBITAL
TRANSFER UNDER THRUST ERRORS, 2**

Antônio Delson Conceição de Jesus
Marcelo Lopes Oliveira e Souza
Antonio Fernando Bertachini de Almeida Prado

Paper presented at the International Conference on Nonlinear Dynamics, Chaos, Control
and Their Applications in Engineering Sciences - ICONNE - 2000.

INPE
São José dos Campos
2001

MONTE-CARLO ANALYSIS OF NONIMPULSIVE ORBITAL TRANSFER UNDER THRUST ERRORS, 2

Antônio Delson Conceição de Jesus

Universidade Estadual de Feira de Santana – UEFS, Feira de Santana, BA, Brasil

Phone/Fax: 55-75-2248085, E-mail: adj@uefs.br

Marcelo Lopes Oliveira e Souza

Instituto Nacional de Pesquisas Espaciais – INPE, São José dos Campos, SP, Brasil

Phone: 55-12-3456201, Fax: 55-12-3456226, E-mail: marcelo@dem.inpe.br

Antônio Fernando Bertachini de Almeida Prado

Instituto Nacional de Pesquisas Espaciais – INPE, São José dos Campos, SP, Brasil

Phone: 55-12-3456201, Fax: 55-12-3456226, E-mail: prado@dem.inpe.br

ABSTRACT

In this paper we studied statistically orbital maneuvers with finite propulsion under thrust errors. We studied two transfer maneuvers: a) a high orbit low thrust coplanar transfer; and b) a middle orbit high thrust noncoplanar transfer (the 1st transfer of the satellite EUTELSAT II-F2). These transfers were done with magnitude and direction (“pitch” and “yaw”) errors in the thrust applied to the satellite. These errors were modeled as random-bias or white noise stochastic processes, with zero mean and unit variance gaussian probability density functions. We studied many cause-effect relations. Among them, the general results suggest that the thrust magnitude errors do not cause appreciable mean final deviations, but that the standard deviation of each thrust direction error holds a nonlinear (almost parabolic) relation with the mean deviation in the final semi-major axis and with the final eccentricity. They suggest and partially characterizes the progressive deformation of the trajectory distribution along the propulsive arc, turning 3sigma ellipsoids into banana shaped volumes curved to the center of attraction (we call them “bananoids”) due to the loss of optimality of the actual (with errors) trajectories with respect to the nominal (no errors) trajectory. A similar deformation but due to initial condition gaussian errors was shown by Junkins. As his plots also suggest, such deformations can not be anticipated by covariance analysis on linearized models with zero mean errors which propagate ellipsoids into ellipsoids always centered in the nominal (no errors) trajectory. Our results also characterize how close or how far are Monte-Carlo analysis and covariance analysis for those examples.

INTRODUCTION

Most space missions need trajectory/orbit transfers to reach their goals. These trajectories/orbits are reached sequentially through transfers between them by changing of its keplerian elements, by firing apogee motors or other sources of force. These have linear and/or angular misalignments that displace the vehicle with respect its nominal directions. The mathematical treatment for these deviations can be realized under many approaches (deterministic, probabilistic, MINMAX, etc.) of the deviations. In the literature, already reviewed by Souza et alli(1998) we highlight:

In the deterministic approach: Schwende and Strobl(1977), Tandon(1988), Rodrigues(1991), Santos-Paulo(1998), Rodrigues and Souza(1999), among others. Related works were done by Rocco(1997) and Schultz(1997).

In the probabilistic approach: Porcelli and Vogel(1980) presented an algorithm for the determination of the orbit insertion errors in biimpulsive noncoplanar orbital transfers(perigee and apogee), using the covariance matrices of the sources of errors. Adams and Melton(1986) extended such algorithm to ascent transfers under a finite thrust, modeled as a sequence of impulsive burns. They developed an algorithm to compute the propagation of the navigation and direction errors among the nominal trajectory, with finite perigee burns. Rao(1993) built a semi-analytic theory to extend covariance analysis to long-term errors on elliptical orbits. Howell and Gordon(1994) also applied covariance analysis to the orbit determination errors and they develop a station-keeping strategy of Sun-Earth L1 libration point orbits. Junkins et alli(1996) and Junkins(1997) discussed the precision of the error covariance matrix method through nonlinear transformations of coordinates. He also found a progressive deformation of the initial ellipsoid of trajectory distribution (due to gaussian initial condition errors), that was not anticipated by the covariance analysis of linearized models with zero mean errors. Carlton-Wipperfurth(1997) proposed differential equations in polar coordinates for the growth of the mean position errors of satellites (due to errors in the initial conditions or in the drag), by using an approximation of Langevin's equation and a first order perturbation theory. Alfried(1999) studied the effects of drag uncertainty via covariance analysis.

In the minimax approach: see russian authors, mainly.

However, all these analyses are approximated. This motivated an exhaustive numerical but exact analysis (by Monte-Carlo), and a partial algebraic analysis done by Jesus(1999) under the supervision of the two other authors, to highlight and to study effects not shown in those analyses.

In this work we present the 2nd part of that Monte-Carlo analysis of the nonimpulsive orbital transfers under thrust vector errors. The results were obtained for two transfers: the first, a low thrust transfer between high coplanar orbits, used by Biggs(1978, 1979) and Prado(1989); the second, a high thrust transfer between middle noncoplanar orbits (the first transfer of the EUTELSAT II-F2 satellite) implemented by Kuga et alli(1991).

The simulations were done for both transfers with minimum fuel consumption. The optimization method used by Biggs(1978, 1979) and Prado(1989) was adapted to the case of the transfers with thrust errors. The "pitch" and "yaw" angles were taken as control variables such that the overall minimum fuel consumption defines each burn of the thrusters.

The error sources that we considered were the magnitude errors, “pitch” and “yaw” directions errors of the thrust vector, as causes of the deviations found in the several keplerian elements of the transfer trajectory. Each deviation was introduced separately along the orbital transfer trajectory. Besides this, we studied two kind of errors for each one these causes: the random-bias and the white-noise errors. The random-bias errors are even errors during the transfer arc, while the white-noise errors change along the transfer arc. These error sources introduced in the orbital transfer dynamic produce effects in the final orbit keplerian elements in the final instant.

In this work we present an statistical analysis of the effects of these errors on the mean of the deviations of the keplerian elements of the final orbit with respect to the reference orbit (final orbit without errors in the thrust vector) for both transfers. The approach that we used in this work for the treatment of the errors was the probabilistic one, assuming these as having zero mean unit variance gaussian probability density function.

MATHEMATICAL FORMULATION AND COORDINATE SISTEMES

The orbital transfer problem studied can be formulated in the following way:

- 1) Globally minimize the performance index: $J = m(t_0) - m(t_f)$;
- 2) With respect to $\alpha : [t_0, t_f] \rightarrow \mathbb{R}$ (“pitch” angle) and $\beta : [t_0, t_f] \rightarrow \mathbb{R}$ (“yaw” angle) with $\alpha, \beta \in C^{-1}$ em $[t_0, t_f]$;
- 3) Subject to the dynamics in inertial coordinates X_i, Y_i, Z_i of Figure 1: $\forall t \in [t_0, t_f]$,

$$m(t) \cdot \frac{d^2 X}{dt^2} = \frac{-\mu m(t) \cdot X}{R^3} + F_x \quad (1)$$

$$m(t) \cdot \frac{d^2 Y}{dt^2} = \frac{-\mu m(t) \cdot Y}{R^3} + F_y \quad (2)$$

$$m(t) \cdot \frac{d^2 Z}{dt^2} = \frac{-\mu m(t) \cdot Z}{R^3} + F_z \quad (3)$$

$$F_x = F [\cos \beta \sin \alpha (\cos \Omega \cos \theta - \sin \Omega \cos I \sin \theta) - \cos \beta \cos \alpha (\cos \Omega \sin \theta + \sin \Omega \cos I \cos \theta) + \sin \beta \sin \Omega \sin I] \quad (4)$$

$$F_y = F [\cos \beta \sin \alpha (\sin \Omega \cos \theta + \cos \Omega \cos I \sin \theta) - \cos \beta \cos \alpha (\sin \Omega \sin \theta - \cos \Omega \cos I \cos \theta) - \sin \beta \cos \Omega \sin I] \quad (5)$$

$$F_z = F (\cos \beta \sin \alpha \sin I \sin \theta + \cos \beta \cos \alpha \sin I \cos \theta + \sin \beta \cos I) \quad (6)$$

$$m(t) = m(t_0) + \dot{m} \cdot (t - t_0), \text{ with } \dot{m} < 0 \quad (7)$$

$$F \equiv |\dot{m}| \cdot c \quad (8)$$

Or in orbital coordinates (radial R, transversal T, and binormal N) of Figure 1:

$$m(t) a_R(t) = F \cdot \cos \beta(t) \cdot \sin \alpha(t) - \frac{\mu m(t)}{R^2(t)} \quad (9)$$

$$m(t) a_T(t) = F \cdot \cos \beta(t) \cdot \cos \alpha(t) \quad (10)$$

$$m(t) a_N(t) = F \cdot \sin \beta(t) \quad (11)$$

$$a_R(t) = \dot{V}_R - \frac{V_T^2}{R} - \frac{V_N^2}{R} \quad (12)$$

$$a_T(t) = \dot{V}_T + \frac{V_R V_T}{R} - V_N \dot{I} \cos \theta - V_N \dot{\Omega} \sin I \cdot \sin \theta \quad (13)$$

$$a_N(t) = \dot{V}_N + \frac{V_R V_N}{R} + V_T \dot{I} \cos \theta + V_T \dot{\Omega} \sin I \cdot \sin \theta \quad (14)$$

$$V_R = \dot{R} \quad (15)$$

$$V_T = R(\dot{\Omega} \cos I + \dot{\theta}) \quad (16)$$

$$V_N = R(-\dot{\Omega} \sin I \cdot \cos \theta + \dot{I} \cdot \sin \theta) \quad (17)$$

$$\theta = \omega + f \quad (18)$$

4) Given the initial and final orbits, and the parameters of the problem($m(t_0)$, c, \dots).

These equations were obtained by: 1) writing in coordinates of the dexterous rectangular reference system with inertial directions $OX_i Y_i Z_i$; the Newton's laws for the motion of a satellite S with mass m , with respect to this reference system, centered in the Earth's center of mass O, with X_i axis toward the Vernal point, $X_i Y_i$ plane coincident with Earth's Equator, and Z_i axis toward the Polar Star approximately; 2) rewriting them in coordinates of the dexterous rectangular reference system with radial, transversal, binormal directions SRTN, centered in the satellite center of mass S; helped by 3) a parallel system with $OX_o Y_o Z_o$ directions, centered in the Earth's center of mass O, X_o axis toward the satellite S, $X_o Y_o$ plane coincident with the plane established by the position R and velocity V vectors of the satellite, and Z_o axis perpendicular to this plane; and helped by 4) the instantaneous keplerian coordinates (Ω , I , ω , f , a , e). These equations were later rewritten and simulated by using 5) 9 state

variables, defined and used by Biggs(1978, 1979) and Prado(1989), as functions of angle s shown in Figure 2.

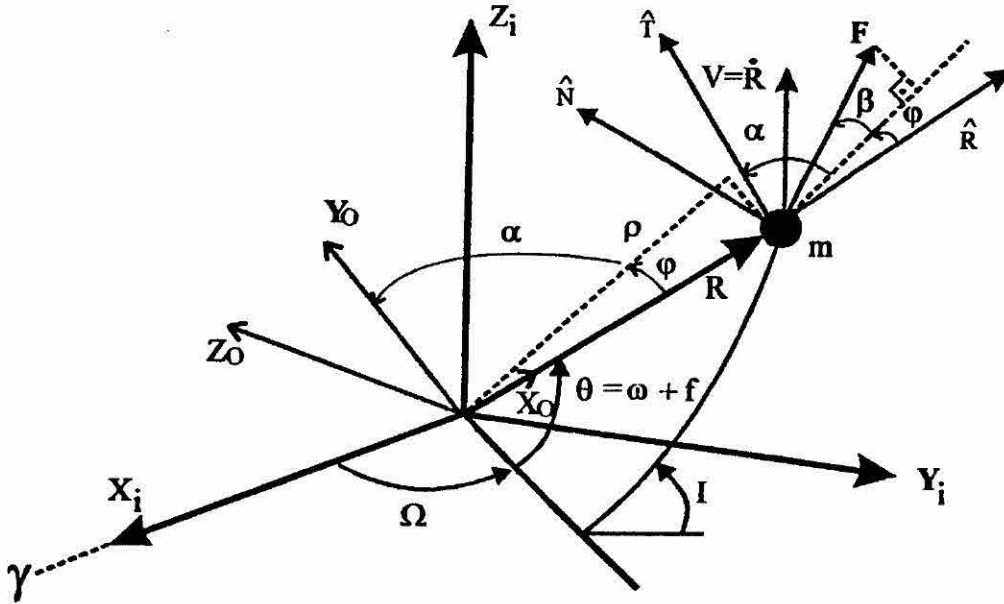


Figure 1 - Reference systems used in this work.

The nonideal thrust vector, with magnitude and direction errors, is given by:

$$\vec{F}_E = \vec{F} + \Delta\vec{F} \quad (19)$$

$$\vec{F}_E = \vec{F}_R + \vec{F}_T + \vec{F}_N \quad (20)$$

$$|\vec{F}_E| = F_E, \quad |\vec{F}| = F \quad (21)$$

$$F_R = (F + \Delta F) \cos(\beta + \Delta\beta) \sin(\alpha + \Delta\alpha) \quad (22)$$

$$F_T = (F + \Delta F) \cos(\beta + \Delta\beta) \cos(\alpha + \Delta\alpha) \quad (23)$$

$$F_N = (F + \Delta F) \sin(\beta + \Delta\beta) \quad (24)$$

where: \vec{F} , \vec{F}_E e $\Delta\vec{F}$ are: the thrust vector without errors, the thrust vector with errors, and the error in the thrust vector, respectively; $\Delta\alpha$ e $\Delta\beta$ are the errors in the “pitch” and in the “yaw” angles, respectively; F_R , F_T e F_N are the components of the thrust vector with errors \vec{F}_E in the radial,

transversal and normal directions, respectively. The magnitude error, ΔF , was computed as a percentage of the nominal force, while the direction errors $\Delta\alpha$ e $\Delta\beta$ were computed in units of angle. They are varied inside given ranges, that is, $\pm \text{DES1.F}$ for ΔF , $\pm \text{DES2}$ for $\Delta\alpha$ and $\pm \text{DES3}$ for $\Delta\beta$. This variation will correspond to the implementation of the random numbers that satisfy a uniform probability distribution into those ranges. In this way, for each implementation of the orbital transfer arc, values of α and β are chosen, whose errors are inside the range, that produce the direction for the overall minimum fuel consumption.

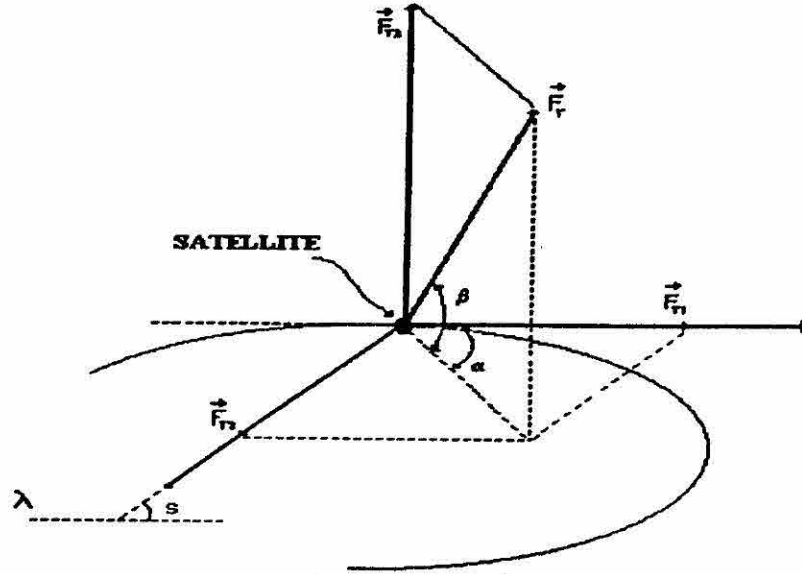


Figure 2 – Thrust vector applied to the satellite and the s variable.

NUMERICAL RESULTS

The simulations were performed with 1000 realizations for each transfer, that is, 1000 runs were done with random values for each DES1, DES2 and DES3, such that the results obtained for the final keplerian elements represent the arithmetic mean of 1000 realizations (mean over the ensemble). The value 1000 was chosen to represent the set of runs because the mean deviations in all final keplerian elements with respect to their references converge to their minima for this number of runs.

Figures 3 and 4 show the mean deviations in the final semi-major axis and eccentricity versus the number of runs, respectively. These plots were done for systematic pitch direction with $\text{DES2}=1,0^\circ$. The computation of the mean deviations of the final keplerian elements with respect to their references can be estimated by the arithmetic mean of them, for 1000 runs as representatives. So, we can estimate mean deviation of any final keplerian element, ΔK as

$$\overline{\Delta K} = E\{\Delta K\} = \int_{-\infty}^{\infty} \xi f_{\Delta K}(\xi) d\xi \equiv \sum_{i=1}^{N=1000} \frac{\Delta K_i}{N} \quad (25)$$

It is important to remark that Eq. (25) estimates a mean in the ensemble and not in the time. In this work we present only these estimates for the final semi-major axis and eccentricity with respect to their

references. Figures 5 to 10 present the behavior of them as functions of the maximum (random-bias and white noise) direction errors.

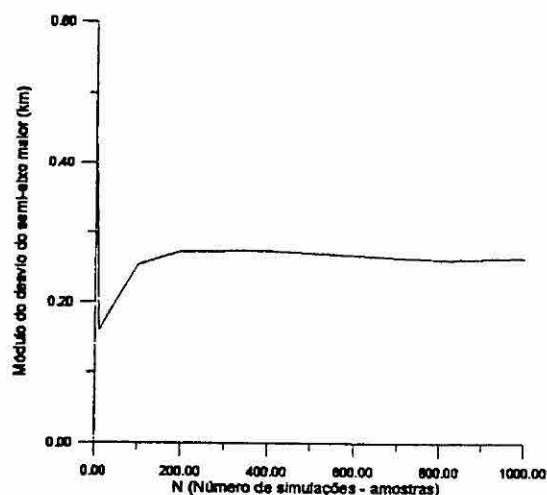


Figure 3 – Semi-major axis deviation vs N

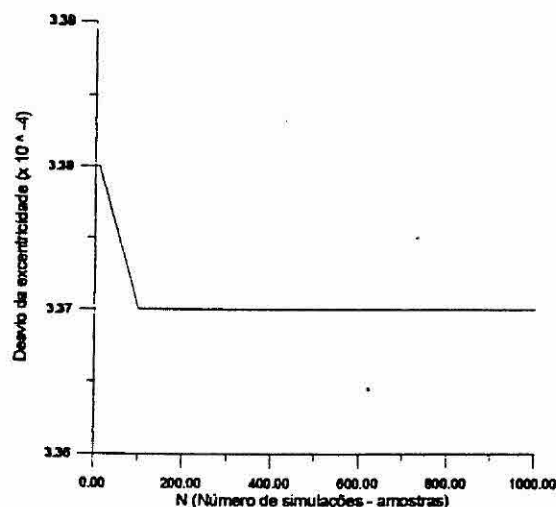


Figure 4 - Eccentricity deviation vs N

1) Semi-major axis (a), Gaussian Random-Bias and White-Noise “Pitch” Errors

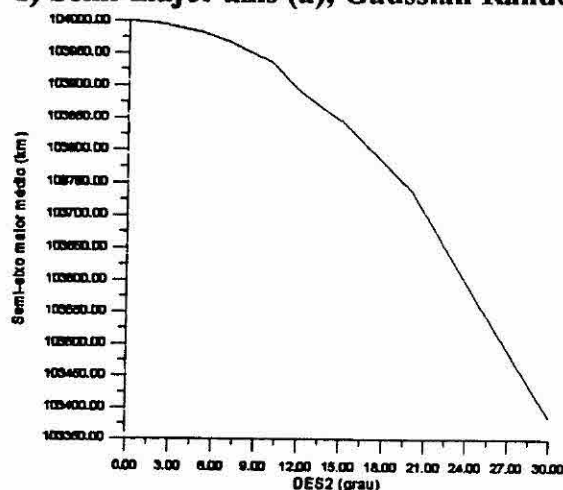


Figure 5 – First Maneuver:
 $E\{a(t_f)\}$ vs DES2

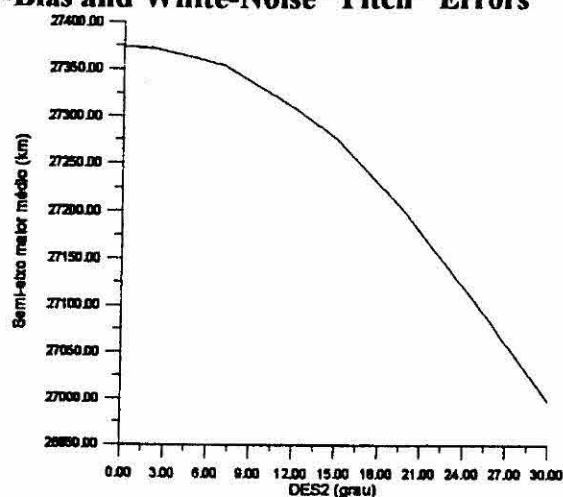


Figure 6 – Second Maneuver
 $E\{a(t_f)\}$ vs DES2

In these plots, we observe behaviors very similar for both maneuvers, although their causes are very different from each other. We easily observe that the values of the mean semi-major axis present a region of decrease sufficiently defined according to the growth of the maximum “pitch” error, DES2. Figure 5 is for a random-bias “pitch” error and Figure 6 is for a white-noise “pitch” error. Both suggest the same nonlinear (almost parabolic) relation not depending of the maneuver studied.

2) Semi-major axis (a), Gaussian Random-Bias and White-Noise “Yaw” Errors

Once more these plots show behaviors well defined and similar for the semi-major axis as function of the maximum “yaw” error, DES3, for both maneuvers studied. That is, there is a region of decrease well defined between the elements a and DES3. Figure 7 shows the result of the random-bias “yaw”

errors and Figure 8 shows the result of the white-noise “yaw” errors. The behaviors are the same for the both cases.

These results show clearly the influence of the white-noise errors when the second maneuver is simulated with errors in “yaw”. The region of decrease still exist, as well as the nonlinear relation, but there are fluctuations in the growth of the maximum “yaw” error.

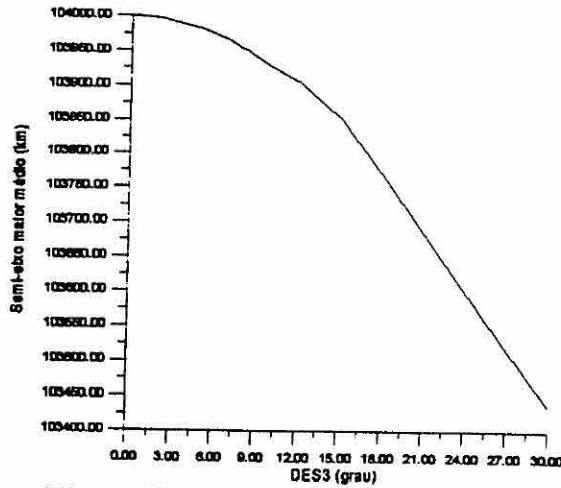


**Figure 7 – First Maneuver:
 $E\{a(t_f)\}$ vs DES3**

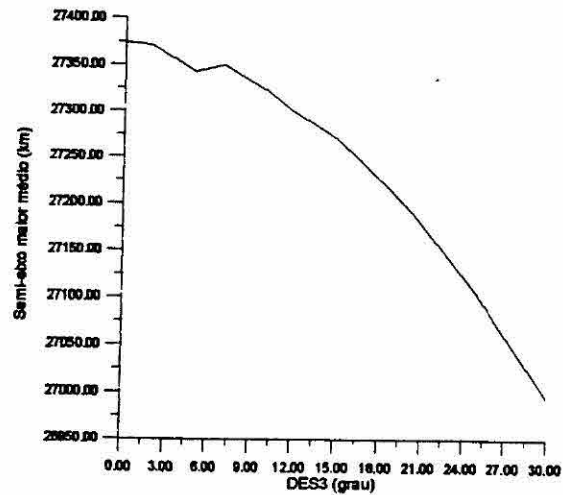


**Figure 8 – Second Maneuver
 $E\{a(t_f)\}$ vs DES3**

3) Eccentricity (e), Gaussian Random-Bias and White-Noise “Pitch” and “Yaw” Errors

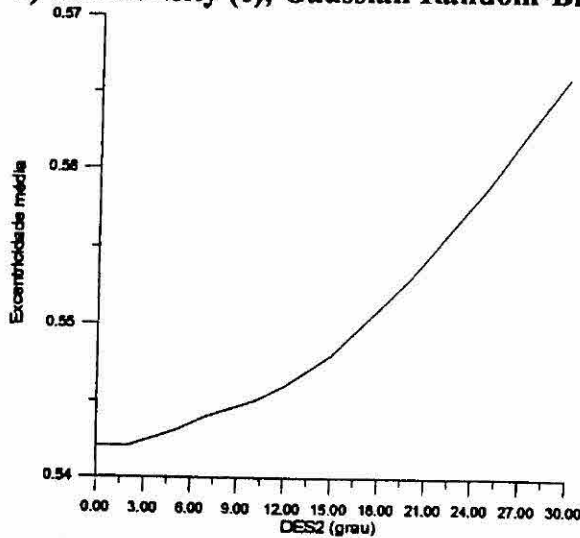


**Figure 9 – Second Maneuver:
 $E\{e(t_f)\}$ vs DES2**

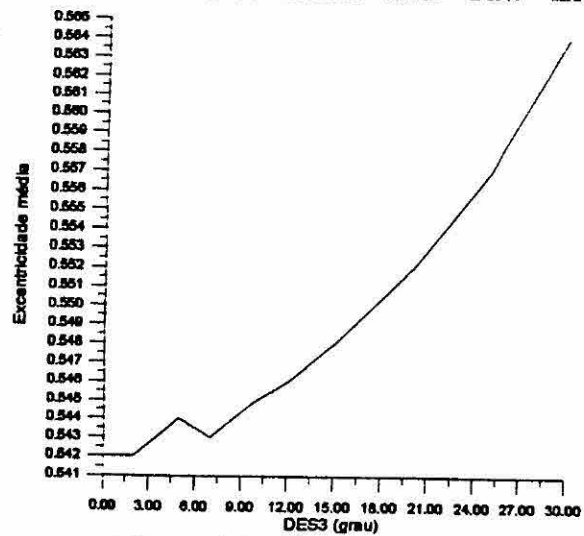


**Figure 10 – Second Maneuver:
 $E\{e(t_f)\}$ vs DES3**

These plots show the nonlinear behavior of the mean deviation in the final eccentricity with the maximum “pitch” and “yaw” deviations. They were done only for the second maneuver because in the first one the change of the eccentricity is close to zero for the usual values of DES2 and DES3. They were plotted with precision of 10^{-3} for the eccentricity.

We observed in the figures that for the white-noise errors the results were very similar to the results obtained for the random-bias errors but, the curves for the “pitch” errors present a more defined pattern with respect to those for the “yaw” errors, where small fluctuations appear in its final form. It is possible to see that the influence of the out-of-plane (“yaw”) errors is so strong in the definition of the orbital transfer trajectory. Figure 9 is for the random-bias “pitch” errors and Figure 10 is for the white-noise “yaw” errors.

The results show that the values of the eccentricity also fluctuate for practical maneuvers with the white-noise errors in “yaw”, but keeping the region of growth similar to the one verified for the random-bias errors case. So, we can say that all these results suggest and partially characterizes the progressive deformation of the trajectory distribution along the propulsive arc. It occurs due to the loss of optimality of the actual trajectories (with errors) with respect to the nominal trajectories (without errors).

The dependence of the final keplerian elements with the magnitude errors for any of the cases was practically null, specially for the mean deviation of the final semi-major axis, since the perturbations occurred in this element were probably due to its estimator and they were comparable to the numerical errors of the experiment, as shown in Figures 11 and 12. They show that the mean deviation in the final semi-major axis is much smaller than the cone $\pm 1 \sigma$ (standard deviation of the deviation in the final semi-major axis).

The values for DES1, DES2 and DES3 used in these plots range from usual values to unusual values, with the aim to verify the general behaviors. Obviously, it is not usual to have a “pitch” error equal to $30,0^\circ$ or a magnitude error equal to 30,0%, for example.

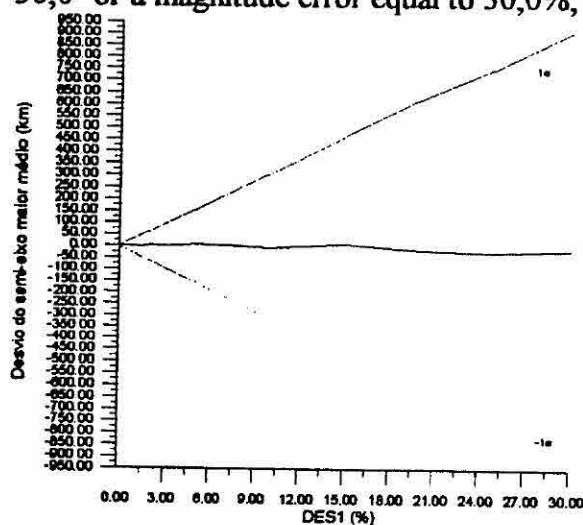


Figure 11 – Theoretical case; Δa vs DES1
 $e \sigma$ (standard deviation)

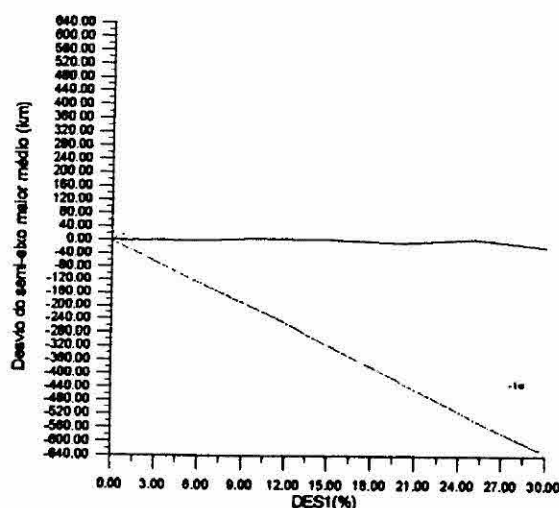


Figure 12 – Practical case; Δa vs DES1
 $e \sigma$ (standard deviation)

CONCLUSIONS

This work presented the influence of gaussian thrust vector errors on nonimpulsive orbital transfer maneuvers. It was verified that, in any case, the mean deviation in the final semi-major axis presents a nonlinear (approximately parabolic) dependence with the maximum error in thrust direction. The same results were verified for the mean deviation in the final eccentricity, for the second transfer. The

respective dependence with the errors in thrust magnitude were not verified. These results are similar to that obtained by Jesus¹³ for the uniform probability density functions of the errors. The general results suggest a progressive deformation of the trajectory distribution along the propulsive arc. This deformation may be associated to the loss of the optimality of the actual trajectories with respect to the nominal trajectory.

REFERENCES

- Adams, N. J., and Melton, R. G. (1986) "Orbit Transfer Error Analysis for Multiple, Finite Perigee Burn, Ascent Trajectories". *The Journal of Astronautical Sciences*, Vol. 34, No. 4, October-December, pp.355-373.
- Alfriend, K. T. (1999) "Orbit Uncertainty Due to Drag Uncertainty". Paper presented at the 14th International Symposium on Spaceflight Systems and Data Control - ISSSDC XIV at Iguassu Falls, Parana, Brazil, February 8-12, 1999.
- Biggs, M. C. B. (1978) "The Optimisation of Spacecraft Orbital Manoeuvres. Part I: "Linearly Varying Thrust Angles". The Hattfield Polytechnic Numerical Optimisation Centre, Connecticut, USA.
- Biggs, M. C. B. (1979) "The Optimisation of Spacecraft Orbital Manoeuvres. Part II: "Using Pontryagin's Maximum Principle ". The Hattfield Polytechnic Numerical Optimisation Centre, Connecticut, USA.
- Carlton-Wipperfurth, K. C. (1997) "Satellite Position Dilution of Precision (SPDOP)". AAS Paper 97-609, presented at the 1997 AAS/AIAA Astrodynamics Specialist Conference, Sun Valley, ID, August 4-7.
- Howell, K. C. and Gordon, S. C. (1994) "Orbit Determination Error Analysis and a Station-Keeping Strategy for Sun-5-Earth L1 Libration Point Orbits". *The Journal of Astronautical Sciences*, Vol.42, No.2, April-June 1994, pp.207-228.
- Jesus, A. D. C. (1999) "Análise Estatística de Manobras Orbitais com Propulsão Finita Sujeita a Erros no Vetor Empuxo". Doctoral Thesis. INPE, São José dos Campos, São Paulo, Brazil.
- Jesus, A. D. C.; Souza, M. L. O. and Prado, A. F. B. (1999) Monte-Carlo Analysis Of Nonimpulsive Orbital Transfer Under Thrust Errors, 1. AAS/AIAA Astrodynamics Specialist Conference, Girdwood, Alaska, USA, August 16-19 (Paper AAS 99-424).
- Junkins, J. L., Akella, M. R., and Alfriend, K. T. (1996) "Non-Gaussian Error Propagation in Orbital Mechanics". *The Journal of the Astronautical Sciences*, Vol. 4, No. 4, October-December, pp.541-563.
- Junkins, J. L. (1997) "Adventures on the Interface of Dynamics and Control". *Journal of Guidance, Control, and Dynamics*, Vol. 20, No. 6, November-December, pp.1058-1071.
- Kuga, H. K., Gill, E., Montenbruck, O. (1991) "Orbit Determination and Apogee Boost Maneuver Estimation Using UD Filtering". DLR-GSOC, Wesling, Germany(Int. Report DLR-GSOC IB 91-2).

- Longuski, J. M., Kia, T., and Breckenridge, W. G. (1989) "Annihilation of Angular Momentum Bias During Thrusting and Spinning-up Maneuvers. *The Journal of the Astronautical Sciences*, Vol. 37, No. 4, October-December, pp.433-450.
- Porcelli, G., and Vogel, E. (1980) "Two-Impulse Orbit Transfer Error Analysis Via Covariance Matrix". *Journal of Spacecraft and Rockets*, Vol. 17, No. 3, pp. 248-255.
- Prado, A. F. B. A. (1989) "Análise, Seleção e Implementação de Procedimentos que Visem Manobras Ótimas de Satélites Artificiais". Master Dissertation. Instituto Nacional de Pesquisas Espaciais (INPE). São José dos Campos, São Paulo (INPE-5003-TDL/397).
- Rao, K. R. (1993) "Orbit Error Estimation in the Presence of Force Model Errors". AAS Paper 93-254, *Advances in the Astronautical Sciences*, Vol. 84, No. 1, pp. 61-74.
- Rocco, E. M. (1997) "Manutenção Orbital de Constelações de Satélites Simétricas com Manobras Impulsivas Ótimas com Limite de Tempo". Doctoral Thesis (on going). Instituto Nacional de Pesquisas Espaciais (INPE), DMC. São José dos Campos/SP- Brasil.
- Rodrigues, D. L. F. (1991) "Análise Dinâmica da Transferência Orbital". Master Dissertation. Instituto Nacional de Pesquisas Espaciais (INPE), São José dos Campos, São Paulo, Brasil (INPE-5352-TDI/461).
- Rodrigues, D. L. F. and Souza, M. L. O. (1999) "Effects of Planar Thrust Misalignments on Rigid Body Motion." *Journal of Guidance, Control, and Dynamics*, vol. 22, No.6, November-December, pp. 916-918.
- Santos-Paulo, M. M. N. (1998) "Estudo da Influência dos Erros dos Propulsores em Manobras Orbitais Tridimensionais". Master Dissertation. Instituto Nacional de Pesquisas Espaciais (INPE). São José dos Campos, SP.
- Schultz, W. (1997) "Transferências Biimpulsivas entre Órbitas Elípticas Não Coplanares com Consumo Mínimo de Combustível". Master Dissertation. Instituto Nacional de Pesquisas Espaciais (INPE), São José dos Campos, SP, Brasil.
- Schwende, M. A. and Strobl, H. (1977) "Bi-propellant Propulsion Systems for Spacecraft Injection and Control", *Attitude and Orbit Control Systems. Proceedings*, ESA, Paris, p.405-412.
- Souza, M. L. O., Prado, A. F. B. A., Rodrigues, D. L. F., Santos-Paulo, M. M. N., Jesus A. D. C. and Rocco, E. M. (1998) "A Discussion on the Effects of Thrust Misalignments on Orbit Transfers", *Proceedings of the XXI Congresso Nacional de Matemática Aplicada e Computacional*, Caxambu, MG, Brasil, September 14-18, pp.73-89.
- Tandon, G. K. (1988) "Modeling Torques Due to Orbit Maneuvers", *Astrophysics and Space Science Library*, 733, p.580-583.